

Distortions of Spherical Data in the Wavenumber Domain

Jeong-Woo Kim and Dong-Cheon Lee

Dept. of Earth Sciences and Research Inst. of Geoinformatics & Geophysics, Sejong University

Abstract : Sampling rates become inconsistent when spatial data in the spherical coordinate are resampled with respect to latitudinal or longitudinal degree for mathematical processes such as Fourier Transform, and this results in distortions of the processed data in the wavenumber domain. These distortions are more evident in the polar regions. An example is presented to show such distortions during the recovery process of free-air gravity anomalies from ERS-1 satellite radar altimeter data from the Barents Sea in the Russian Arctic, and a method is presented to minimize the distortion using the Lambert Conformal Conic map projection. This approach was found to enhance the free-air gravity anomalies in both data and wavenumber domains.

Key Words : Fourier Transform, Data Distortions, Map Projection, Gravity Anomalies.

1. Introduction

In general, spatial data acquired from satellite, airborne, and shipborne geophysical surveys have latitude(ϕ), longitude(λ), and altitude(r) coordinate systems, and, hence, the spherical coordinate is often used for data processing. In order to adapt Fast Fourier transform (FFT) for mathematical data processing, for example, a resampling procedure is required in the spherical coordinate to make the number of spherical data set a power of two. The resampled data then have consistent angular increments in longitudinal and latitudinal axes, but the actual surface distances between the data points are not the same, particularly in the longitudinal axis. This results in unnecessary distortion in the FT because a uniform sampling rate (frequency/cycle) is strongly required for calculating accurate

wavenumber.

In this study, the above-mentioned distortion of the spherical data was examined using ERS-1 satellite radar altimeter data from the Barents and Kara Seas in the Russian Arctic (20° - 70° E and 68° - 78° N). Geoid undulations (GU) were first extracted from the satellite radar altimeter data by Kim(1996)'s approach and converted to the free-air gravity anomalies (FAGA) using the Fundamental Equation of Geodesy and Brun's Formula (Heiskanen and Moritz, 1967), in the wavenumber domain. During this procedure, such a distortion was expected to occur. The Lambert Conformal Conic Projection (LCCP) was then applied in order to reduce spatial distortions. The LCCP was used to project the spherical (ϕ , λ) data to the planar (X, Y) coordinate to calculate the accurate wavenumber in the FT. The result was compared with other

independently estimated global FAGA by Anderson and Knudsen(1998) and with shipborne FAGA(NGDC, 1998).

2. Recovery of Free-Air Anomalies from ERS-1 Altimeter Data

In this section, procedures for recovering free-air gravity anomalies (FAGA) from ERS-1 168-day mission data (OPR-2 format) are briefly discussed. The complete data were analyzed to compile FAGA for the Barents and Kara Seas in the Russian Arctic (20°–70° E and 68°–78° N). However, the FAGA between 40°–50° E and 70°–76° N are used for data comparison. Total 115309 ascending and 116163 descending measurements were analyzed to extract GUs for the study area.

There are two different approaches for deriving FA gravity anomalies from satellite altimetry. In the first approach, vertical deflections of the undulation data are used to calculate FAGA (Sandwell and McAdoo, 1988). The benefit of this approach is ostensibly that it is not necessary to do orbital and cross-over adjustment, because the gradient solutions are being used. However, this approach distorts the regional anomalies that may be important in studying large-scale crustal features, and includes track noise in its predictions. The other approach, developed by Kim (1996), derives solutions directly from GUs using the fundamental equation of geodesy and Brun's formula (Heiskanen and Moritz, 1967). This method incorporates orbital cross-over adjustments and spectral correlation filtering of neighboring orbital data as well as maps from ascending and descending data sets to obtain the best possible estimate of the geoidal undulation. This approach enhances the recovery of gravity anomalies at all wavelengths because it is based on determining GUs as accurately as possible. Furthermore, this approach permits procedures to be implemented in the frequency

domain that are effective for minimizing track noise, especially at high latitudes where ascending and descending orbits cross each other at high angles (Kim *et al.*, 1998). Because of these relative advantages, the second method by Kim (1996) was used for recovering FAGA in this study.

Two key concepts permit effective determination of GU data from satellite altimetry. The first concept is that the sea surface is approximately equivalent to the geoid. The second concept is that the orbit of the satellite altimeter is measured in ellipsoidal coordinates (i.e., the satellite orbital elevation is with respect to the Earth's ellipsoid). Therefore, when the satellite's elevation is differenced with the height above the ocean, the difference is approximately equal to the GU. Corrections for atmospheric effects and sea surface variability to estimate more accurate geoid surface are also applied based on direct observations and models.

From the derived GUs, the FA gravity anomalies may be estimated because both quantities are related to the disturbing potential T. GUs are related to the disturbing potential through Brun's formula (Heiskanen and Moritz, 1967)

$$T = N \gamma, \quad (1)$$

where N is GU in cm; T is disturbing potential in gal.cm; and γ is normal gravity in gal. The disturbing potential T represents the gravitational potential of the mass that deviates from a standard (homogeneous) model (such as the ellipsoidal earth). These inhomogeneities in the earth's structure are represented by proportional changes in the GU. Gravity anomalies are also related to the disturbing potential through the fundamental equation of geodesy (Heiskanen and Moritz, 1967)

$$\Delta g = -\partial T / \partial r - 2T/R, \quad (2)$$

where (Δg is gravity anomaly in gal; R is the radius of the earth in cm; and r is the displacement vector. The first term in Eq. (2) is the gravity disturbance and the

second term represents a correction term for the GU. Both terms are functions of the disturbing potential that is determined by Eq. (1) from the derived GU data.

Therefore, in recovering the FA gravity anomalies from altimetry data, it is very important to determine accurate GUs from the altimetry observations. The FAGA will be directly calculated from the vertical derivative of the GUs (i.e., Eq. (2)).

Kim(1996) then generated the residual FA gravity anomalies using Eqs. (1) and (2) from the GUs. He calculated the radial derivatives with FFT in spherical coordinates (ϕ, λ) , assuming the spherical coordinate data had approximately the same station spacing in km in each direction. This assumption may result in unnecessary distortions particularly in the high latitude region. In this paper, therefore, the GUs were transformed to an (X, Y) plane using a Lambert Conformal Conic Projection. Then the vertical derivative was taken to generate residual FA gravity anomalies and projected back into spherical coordinates (ϕ, λ) .

3. Wavenumber in the Fourier Transform

The Fourier transform (FT) is a basic ingredient of geophysical signal analysis. The FT applies to various types of geopotential data processing such as power spectrum analysis, derivatives, continuation, wavenumber correlation analysis (von Frese *et al.*, 1997), and spectral noise reduction of survey track-line (Kim *et al.*, 1998).

In the FT, wavenumber (κ) is inversely proportional to wavelength (η) ($\eta \propto (1/\eta)$), and wavenumber κ physically means the uniform sampling rate, i.e., the constant frequency per cycle. Calculating the accurate number of κ , therefore, depends entirely on the sampling rate or the distance between the sampling points. However, the resampled data in the spherical coordinate using longitude and latitude increments

eventually have the same degree (i.e. angular) increments, and hence, the distance between the resampled points are not consistent.

The distance (y) between the two points at the different longitudes on a same latitude(ϕ) is different from the distance between the two points at the same longitudes on a different latitude(ϕ') with a relationship of

$$y' = y \cos(\phi' - \phi)^\circ. \quad (3)$$

Quantitatively, y' decreases about 0.015% when ϕ' moves 1° toward the pole (15m/100km), and this effect increases as we approach the pole. This results in systematic errors in calculating κ , and, as a result, distortions of the processed data when inversely transformed to the spatial domain. To minimize these unnecessary distortions, the sampling rates need to be consistent, and one of the solutions is projecting the spherical data to the (X, Y) plane using a proper map projection such as Lambert Conformal Conic Projection so that the distance between the points is consistent.

4. Lambert Conformal Conic Projection

A map projection is a systematic representation of all or part of the surface of a round body, especially the Earth, on a plane. More specifically, a map projection is a procedure of converting a point in the datum plane (ϕ, λ) to a projection plane (X, Y) . The Lambert Conformal Conic Projection (LCCP), developed by Lambert in 1772, is mathematically based on a cone that is tangent at one parallel, or, more often, conceptually secant on two the parallels (Snyder, 1987; Alpha and Snyder, 1982).

In the LCCP, lines of longitude in the LCCP (i.e., meridians) are straight lines converging at the pole, while lines of latitude (i.e., parallels) are arcs of concentric circles concave toward a pole and centered at

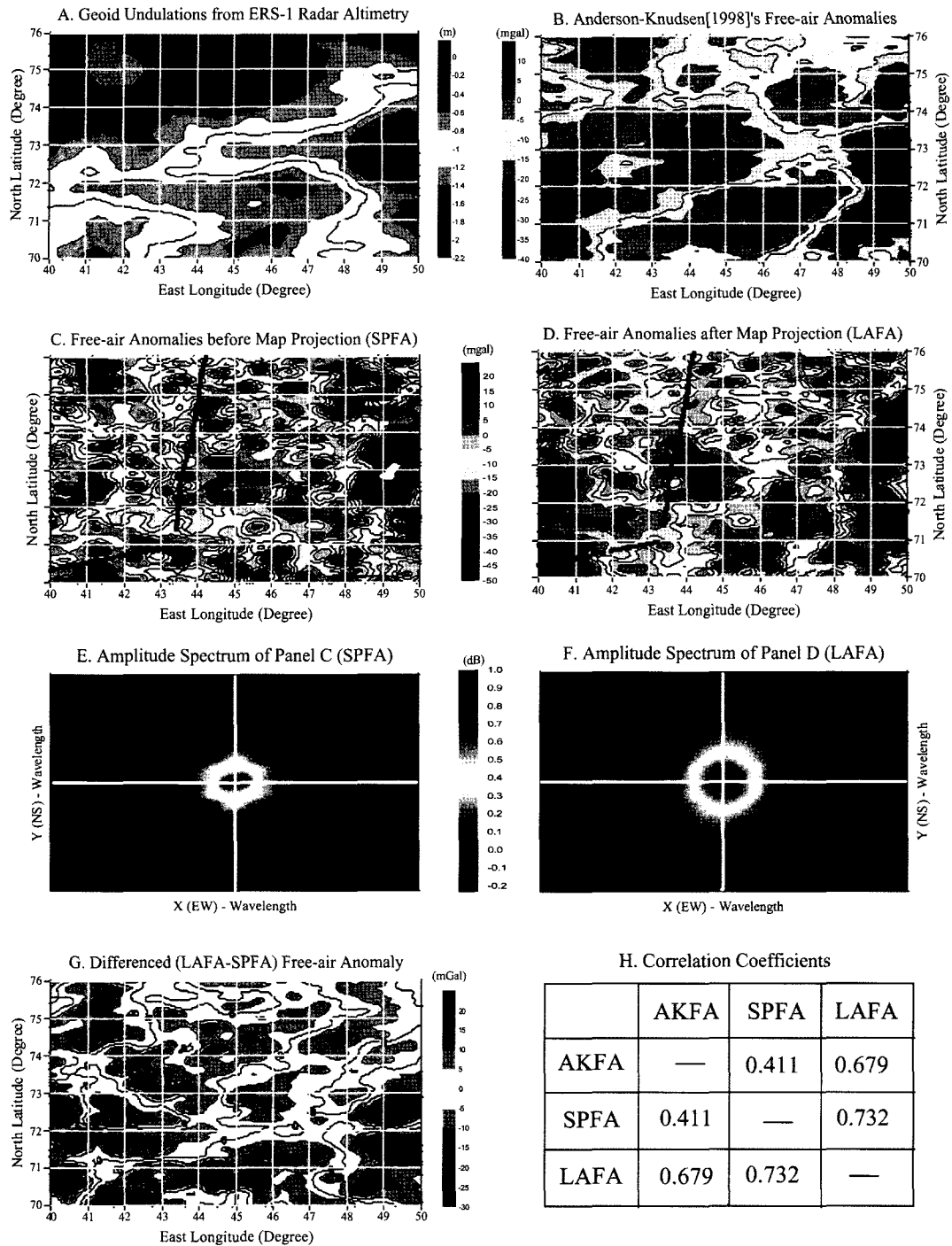


Fig. 1. Geoid undulations (A) and free-air gravity anomalies before (C) and after (D) Lambert Conformal Conic Projection from ERS-1 satellite radar altimetry. The anomalies in C and D are compared with the Anderson-Knudsens(1998)'s model shown in B. Panels E and F are the amplitude spectra of C and D, respectively. Panel G shows the differences between C and D. The Correlation Coefficients between the data are shown in H.

the pole. Meridian spacing is true on the two standard parallels and decreases toward the pole, and parallel spacing increases away from the standard parallels and decreases between them. Meridians and parallels intersect each other at right angles. Areal distortion, therefore, is minimal but increases away from the standard parallels (Szava-Kovats, 1964). The LCCP is used for large areas in the mid-latitudes having an east-west orientation. For example, the U.S. (50 states) Base Map uses standard parallels at 37°N and 65°N.

Since Fourier transform requires uniform sampling distance, FT was performed on the 2D projected plane - generated by LCCP - with equal sampling distance. Other map projections may be applied, however, LCCP with two standard parallels provides minimum geometric distortion for both longitudinal and latitudinal directions because the scale is true along the standard parallels and all meridians. Therefore, the scale factors in the overall projected areas are closer to 1, and this value is more optimal than the scale factor from other map projections such as cylindrical and azimuthal map projections.

Accordingly, LCCP was used in this paper because distortion of shapes and areas is minimal, particularly between the standard parallels, as was mentioned above. Standard parallels of 71° and 75°N were selected, because the target area is between 40°-50°E and 70°-76°N in the central Barents Sea of the Russian Arctic. The GUs of spherical coordinate (Fig. 1A) were first projected onto the (X, Y) plane using LCCP, calculated FAGA using Eqs. (1) and (2), and then projected back onto the (ϕ , λ) coordinate (Fig. 1D).

As was mentioned earlier, an extended area of 20°-70°E and 68°-78°N was selected to calculate FAGA for the study area not to be trimmed out and to avoid edge effect during the data processing. Fig. 2 shows the coordinates of the study area before and after LCCP. When the center point of the study area (73°N, 45°E) is considered (0, 0) in the projection plane, the

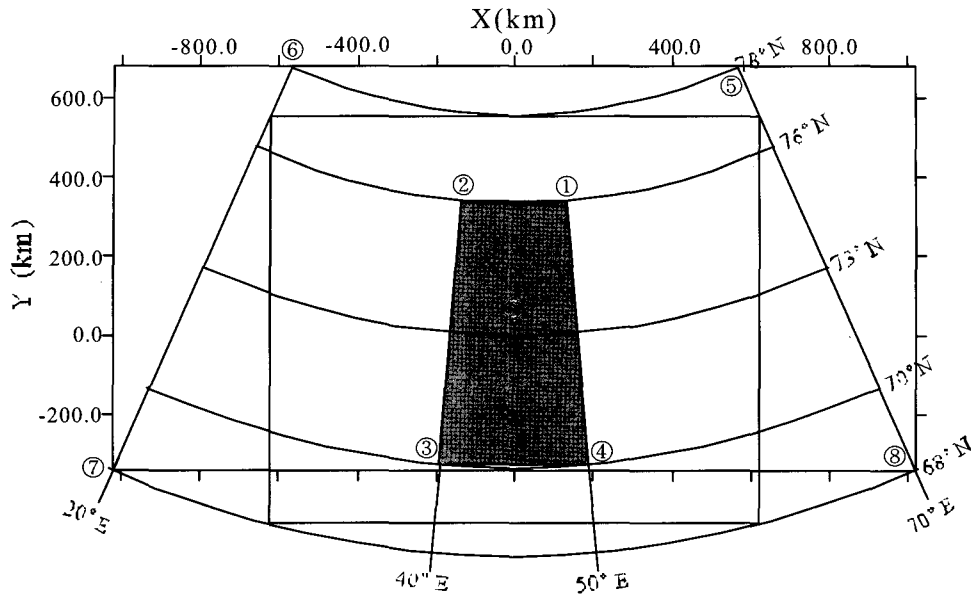
corners of the two study areas (①~⑧) are then converted as shown in the lower panel. The unit of the projected coordinates is Km, and the GUs of the shaded area was actually resampled with uniform distances in X and Y directions and used to calculate FAGA. To estimate the distortions during the FT, GUs in the spherical coordinate (Fig. 1A) were also Fourier transformed to calculate FAGA and the result is shown in Fig. 1C.

5. Results

The geoid undulations (GUs) of the Barents Sea extracted from ERS-1 168-day mission satellite radar altimeter data are shown in Fig. 1A. The unit of GUs is meter, and the (min, max), (mean), and (standard deviation) are (-2.15, 0.12), -0.81, and 0.39, respectively. From the GUs, FAGA were calculated using Eqs. (1) and (2). FAGA in Fig. 1C were calculated from GUs in the spherical coordinate without map projection (SPFA), while FAGA in Fig. 1D were calculated from projected GUs using Lambert Conformal Conic Projection (LAFA). The LAFA was applied to minimize distortions due to inconsistent sampling rates.

The correlation coefficient (CC) between SPFA and LAFA is 0.732, but means and standard deviations are -2.0, -12.9, and 16.9, 10.6, respectively. These statistical differences are considered to be from projection. Because of this, normalized SPFA and LAFA shown in Fig. 1 for graphic comparison.

The SPFA and LAFA were then compared with Anderson and Knudsen(1998)'s anomalies (AKFA) that were compiled from a more comprehensive data set including Geosat data. AKFA of the study area are shown in Fig. 1B. The CCs between SPFA and LAFA are 0.41 and 0.68, respectively, and this means the LCCP increases the CC of about 65.9%. The CCs are



No.	(ϕ, λ) in degree	(X, Y) in km
①	(73, 45)	(0, 0)
②	(76, 40)	(-135.04, 340.44)
③	(70, 40)	(-190.86, -326.73)
④	(70, 50)	(190.86, -326.73)
⑤	(78, 70)	(565.83, 678.37)
⑥	(78, 20)	(-565.83, 678.37)
⑦	(68, 20)	(-1018.49, -342.52)
⑧	(68, 70)	(1018.49, -342.52)

Fig. 2. Coordinate system of the study area before and after Lambert Conformal Conic Projection (LCCP). When the center point of the study area (73°N, 45°E) is considered (0, 0) in the projection plane, the corners of the two study areas (①-⑧) are then converted as shown in the lower panel. The unit of the projected coordinates is km.

summarized in Fig. 1H. Also (of AKFA (8.44) is much closer to that of LAFA than SPFA.

The amplitude spectrum of SPFA and LAFA were also analyzed to see if any systematic noise is apparent in the frequency domain. These resultant spectra are shown in Fig. 1E and 1F, and the units are dB. While the strong NW-SE washboard effects are found (Kim *et al.*, 1998) in both spectra, no NE-SW effects are found in

Fig. 1F. Also, Fig. 1E (spectrum of SPFA) has more energy in all four quadrant than Fig. 1F (spectrum of LAFA). This means that SPFA have more directional, systematic noise than LAFA in the data domain. The map projection at least partially eliminated one direction of washboard noise in the data processing. This needs to be further studied why only one directional noise was reduced. The differenced anomalies (LAFA-SPFA)

shown in Panel G do not have any systematic components or noise.

Finally, SPFA, LAFA, and AKFA were compared with shipborne gravity acquired by Lamont-Doherty Earth Observatory in August of 1973 (NGDC, 1998). The survey lines are shown in black in Fig. 1C and 1D and named SHIP1 (N-S) and SHIP2 (short, E-W) for analysis. There are 190 and 46 measurements in the SHIP1 and SHIP2, respectively. Panel A of Fig. 3 shows four different anomaly profiles along the SHIP1 and SHIP2, and their CCs are summarized in Panel B. It was found that AKFA are very well correlated with shipborne gravity ($CC > 0.93$), meaning AKFA are reliable. LAFA are relatively well correlated with SHIP1 ($CC = 0.82$) and SHIP2 (0.95), while SPFA have lower

CCs with both SHIP1 (0.70) and SHIP2 (0.05). In particular, SPFA along SHIP2 do not show any coherency with other profiles. In summary, LAFA are better correlated with shipborne gravities and AKFA, in general, than SPFA.

VI. Discussions and Conclusions

In general, spatial data acquired from satellite, airborne, and shipborne geophysical surveys have coordinates of latitude(ϕ), longitude(λ), and altitude(r), and, hence, the spherical coordinate is often used for data processing. These data are often resampled in the spherical coordinate for further mathematical processing

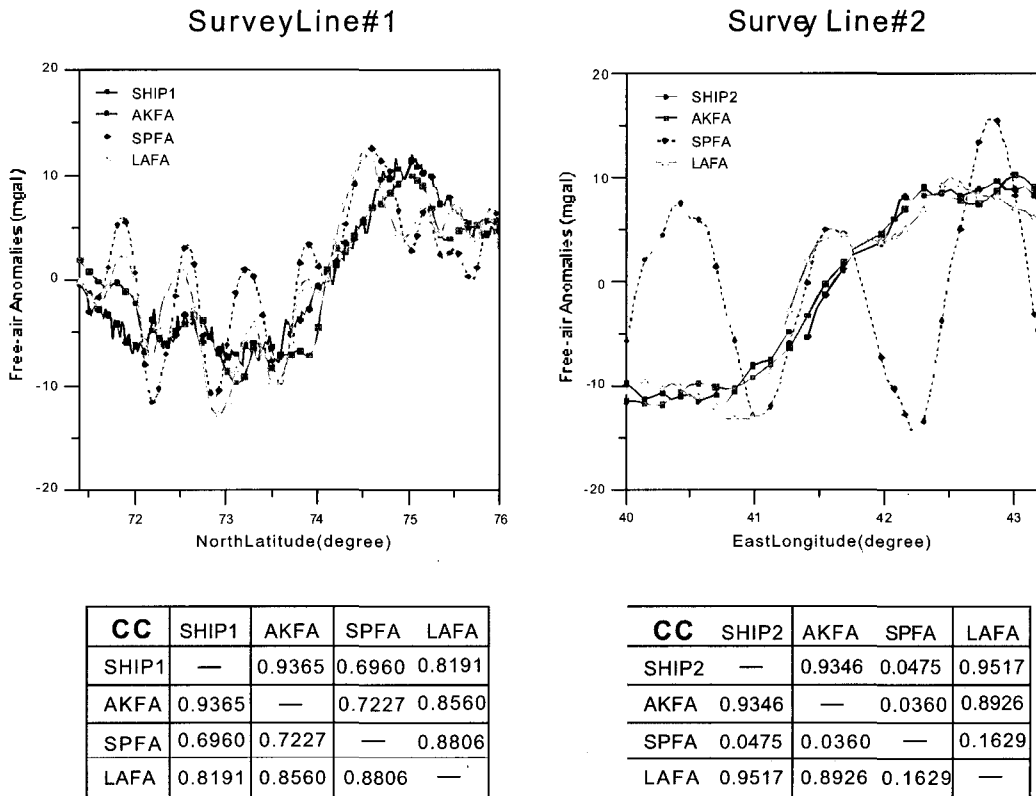


Fig. 3. Comparison of altimetry-implied free-air gravity anomalies and shipborne anomalies. Left and right panels are for survey line #1 (SHIP1) and survey line #2 (SHIP2), respectively.

such as Fourier transform. However, the resampled data in the spherical coordinate using longitude and latitude increments eventually have same degree increments, and hence, the distance between the resampled points are not consistent.

This results in systematic errors of calculating wavenumbers, and as a result, distortions of the processed data in the spatial domain. To minimize these unnecessary distortions, Lambert Conformal Conic Projection was applied to the spherical data so that the distances between resampled points are consistent.

For an example, the distortions occurred during the Fourier transform to calculate FAGA from GU extracted from ERS-1 radar altimeter data from the Barents Sea in the Russian Arctic. The Lambert Conformal Conic Projection was used to minimize the distortion due to inconsistent sampling rate by comparing the result with another global model (Anderson and Knudsen, 1998) and shipborne gravity. This approach was found to enhance the FAGA in both data and wavenumber domains.

Although other map projections may be applied for the same purpose, LCCP was used in this study because LCCP with two standard parallels provides minimum geometric distortion for both longitudinal and latitudinal. The scale factors in the overall projected areas are closer to 1, and this value is more optimal than the scale factors from other map projections such as cylindrical and azimuthal map projections.

However, computational errors and edge effect, as well as loss of the data edge during the transform also occurred during this approach. Also, based on the location and scale of the study area, a proper map projection should be selected carefully. In particular, the azimuth of ground tracks of polar-orbiting satellite are changed greatly near the pole, and the significant distortion will be produced when the data are resampled in the spherical domain using longitude and latitude for Fourier transform (Alsdorf *et al.*, 1994).

Acknowledgments

This work was supported by grant No. R01-2001-00073 from the Korea Science & Engineering Foundation.

References

- Alpha, T.R. and J.P. Snyder, 1982. The properties and uses of selected map projections, Miscellaneous Investigations Series, Map I-1402, USGS, US Dept. of Interior.
- Alsdorf, D.E., R.R.B. von Frese, J. Arkani-Hamed, and H. Noltimier, 1994. Separation of lithospheric, external, and core components of the polar geomagnetic field at satellite altitude, *J. Geophys. Res.*, 99: 4655-4667.
- Anderson, O.B., and P. Knudsen, 1998. Global marine gravity from the ERS-1 and Geosat geodetic mission altimetry, *J. Geophys. Res.*, 103(C4): 8129-8138.
- Blakely, R.J., 1995. Potential theory in gravity and magnetic applications, Cambridge University Press.
- Heiskanen, W.A. and H. Moritz, 1967. Physical Geodesy, W.H. Freeman and Company, 364p.
- Kim, J.W., 1996. Spectral correlation of satellite and airborne geopotential field measurements for lithospheric analysis, Ph.D. Dissertation (unpubl.), Dept. of Geological Sciences, The Ohio State University, 171p.
- Kim, J.W., W.K. Kim, and H.-Y. Kim, 2000. Wavenumber correlation analysis of geopotential anomalies, *J. Korea Econ. Environ. Geol.*, 33(2): 111-116.
- Kim, J.W., J.-H. Kim, R.R.B. von Frese, D.R. Roman, and K.C. Jezek, 1998. Spectral attenuation of

- track-line noise, *Geophys. Res. Lett.*, 25(2): 187-190.
- NGDC, 1998. Marine trackline geophysics data cd-rom set.
- Sandwell, D.T. and D.C. McAdoo, 1998. Marine gravity field of the Southern Ocean and Antarctic margin from Geosat, *J. Geophys. Res.* 93(B9): 10389-10396.
- Snyder, J.P., 1987. Map projections - A working manual, U.S. Geological Survey Professional Paper 1395, U.S. Government Printing Office, Washington.
- Szava-Kovats, G.S., 1964. Notes for an introductory course in map projections, Dept. of Geodetic Science, The Ohio State University.
- von Frese, R.R.B., W.J. Hinze, L.W. Braile, and A.J. Luca, 1981. Spherical earth gravity and magnetic anomaly analysis by equivalent point source inversion, *Earth Planet Sci. Lett.*, 53: 69-86.
- von Frese, R.R.B., M.B. Jones, J.W. Kim, and J.-H. Kim, 1997. Analysis of anomaly correlations, *Geophysics*, 62(1): 342-351.